13th International Conference on CANDU Fuel
Holiday-Inn Waterfront Hotel
Kingston, Ontario, Canada, 2016 August 15-18

MICROSCOPIC EXAMINATION OF UNIRRADIATED CANDU FUEL FROM DARLINGTON NUCLEAR GS

K. Ellison[1], J. Judah[2] , R. Van Lochem[3] and C. Banica[4]
[1]Kinectrics Inc, 800 Kipling Ave, Unit 2, Toronto, Ontario, M8Z 5G5
Ph: 416-207-6000 x 6314, Keith.Ellison@Kinectrics.com)
[2]Consultant –Darlington NGS, Canada
[3]Stern Laboratories Inc., Hamilton, Ontario, Canada
[4] Ontario Power Generation, Darlington NGS, Canada

ABSTRACT – Between 2010 and 2014, Darlington NGS experienced an increase in the number of fuel defects. Elements from unirradiated CANDU fuel bundles manufactured in 2012 and 2013 were disassembled, inspected, and compared with elements manufactured circa 2002. These inspections revealed fractured fuel pellets, debris, and internal damage to the fuel sheaths that may have been caused during pellet loading. The fractured fuel pellets and damaged sheaths were examined in detail to characterize the material damage mechanisms and investigate the underlying causes. Differences in fuel pellet fracture modes were related to variations in UO_2 microstructure, which is typically controlled by the UO_2 powder feedstock, die compaction and sintering process parameters. The OPG investigation identified that the majority of fuel defects were confined to two manufacturing clusters. The focus of this paper is on the benefits of microscopic examinations of fresh fuel.

Introduction

Between 2010 and 2014, Darlington NGS experienced an increase in the number of fuel defects [1]. OPG has conducted an investigation into the cause of this issue and contacted Kinectrics to provide a forensic examination of some fractured, unirradiated uranium dioxide (UO_2) fuel pellets and recovered debris, fuel element sheaths and end caps. The CANDU fuel components supplied for this investigation were from four fuel bundles that were recently disassembled and inspected at Stern Laboratories. As a result of the data collected from the Stern Laboratories several pellets and sheaths were sent to Kinectrics for further examination. This report presents the most important results from the forensic analysis by presenting selected results from three bundles labelled as A, B, and C that were manufactured in 2013, 2012, and 2002, respectively.

1. Fuel Pellet Specimens, Analysis Objectives, and Inspection Methods

Three of the examined pellets were from Bundle A and displayed large fractures or voids on the sides of the cylinders. Two UO_2 fuel pellets were from Bundle B. The majority of the pellets in this element were intact, however both of these pellets contained chips. Finally, two UO_2 fuel pellets were obtained from Bundle C. The majority of the pellets in this bundle were intact, however these two pellets were discovered to be cracked. The analysis objectives were to examine the main fracture surfaces and underlying pellet microstructure for evidence of the mechanism(s) that may have caused the fractures. The damaged fuel pellets were examined visually (with the aid of a stereoscope), by scanning electron microscopy, and via the preparation of polished cross-section specimens for optical metallography.

2. Results

Figure 1 presents images of recently manufactured Pellets 25 and 26 from Element 16, Bundle A. These pellets displayed aligned fractures with rounded chips on one side of each cylinder. Fractures started at the ends (rims) of the cylinders and propagated in predominantly axial directions. Pellet 25 displayed a single main fracture feature that extended approximately 2/3 of the total length of the cylinder. Pellet 26 displayed two fractures that started at opposite ends of the pellet, propagated towards each other in the axial direction, and then converged near the middle of the cylinder. The latter fracture type is sometimes referred to as a 'spoon' shaped fracture. The general directions of primary and secondary crack growth, as determined from the patterns of Wallner lines and velocity hackle [2], are indicated by the yellow arrows. The origin area of the primary fractures were located at the rims of the cylinders within regions of edge chipping. When the pellet fragments were re-assembled, it was noted that there were gaps on either side of the origins, signifying that smaller fragments of debris had been liberated as a result of the fracture mechanism.

Figure 2 presents images of another pellet from Bundle A, Element 16 (Pellet 11). This pellet displayed a U-shaped linear feature at one of the cylinder ends, initially described as a 'tunnel' or 'U-shaped void'. The preliminary visual inspections revealed that the orientation of this U-shaped feature was similar to the edge cracks and chips identified in Pellets 26 and 26. Figure 3 presents SEM images of the U-shaped defect in Pellet 11. This inspection revealed that the edges of the U-shaped feature were sharp and crack-like. At this stage it was recognized that the U-shaped feature was actually a large crack that had not propagated to the same extent as those displayed in Figure 1. The crack origin was centred on the rim of the cylinder in an area that displayed multiple, overlapping edge chips. Detailed SEM examinations revealed a network of secondary cracks in this area of the rim / end face of the cylinder that branched outward to the edge of the cylinder. This resulted in the breakout of small pieces of the pellet. The exposed edges of the U-shaped feature were 'open' with gaps between the fracture faces that were created by the break-out of material. The material break-out was caused by micro-crack convergence. The UO_2 displayed a mixture of transgranular and intergranular fracture. The fracture surface also displayed numerous, intragranular and intergranular voids.

Figure 4 displays polished cross-section images of Pellet 10 from Bundle B, Element 5, which was manufactured in 2012. This pellet displayed macroscopic damage features that were in many ways similar to those just described for Pellets 11, 25, and 26 from Element 16, Bundle A. That is, multiple shallow cracks formed near the inner edge of the rim of the pellet and then propagated axially down the side of the cylinder. The axial cracks emerged at different axial positions, resulting in break-out of several pieces of UO_2. However, in spite of its condition, this pellet and most of the others removed from element B were judged to be relatively intact, compared to those removed from Element A. Pellet 12 from Element 5 also had some large chips, one of which is very similar to Bundle A, Element 16. The SEM examinations of Pellet 10 revealed the presence of numerous secondary cracks and edge chips around the origin area. On a microscopic level, the fracture surfaces displayed a mixture of transgranular and intergranular fracture. The cross-section views displayed in Figure 4 were made through the fracture origin area and propagation zone of Pellet 10. Long secondary cracks can be seen running parallel to, but below the main fracture surface. The secondary cracks were not associated with any specific pre-existing feature of the UO_2 pellet microstructure. On the other hand, the pellet displayed a relatively uniform distribution of voids (dark areas).

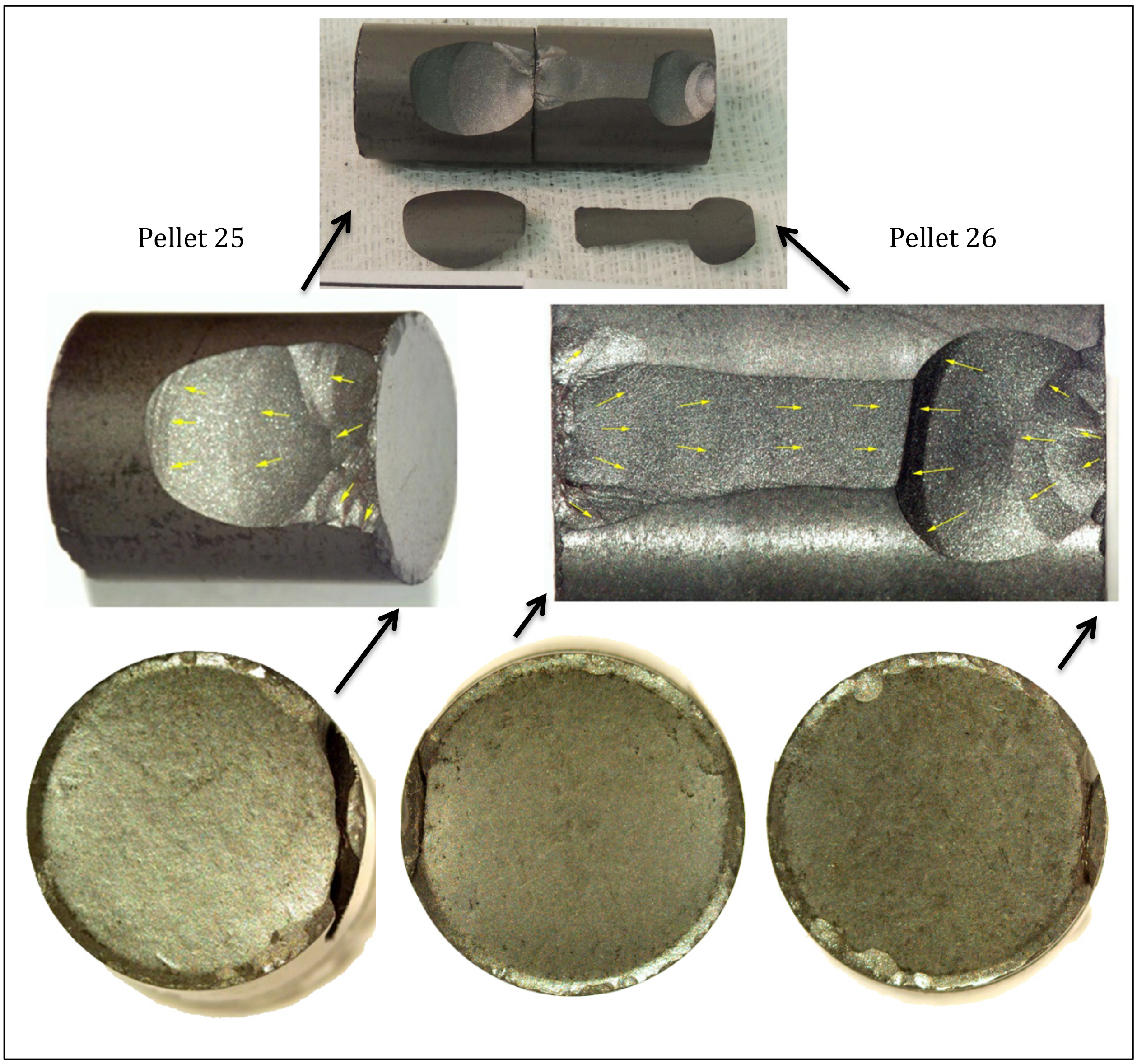

Figure 1 Crack origin areas (OA) and propagation directions (arrows) for Pellets 25 and 26 from Element 16, Bundle A.

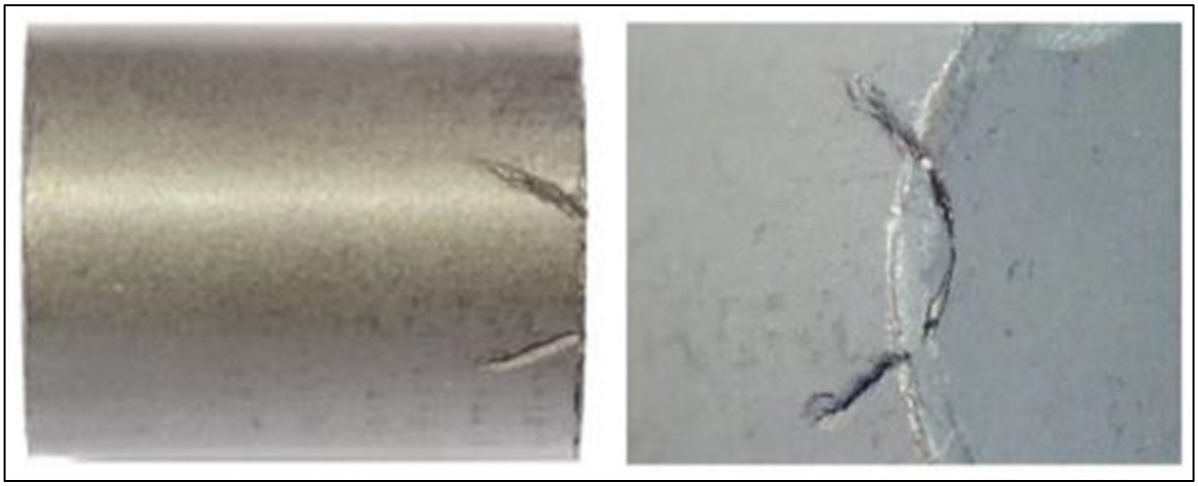

Figure 2   A U-shaped defect in Pellet 11 from Bundle A, Element 16.

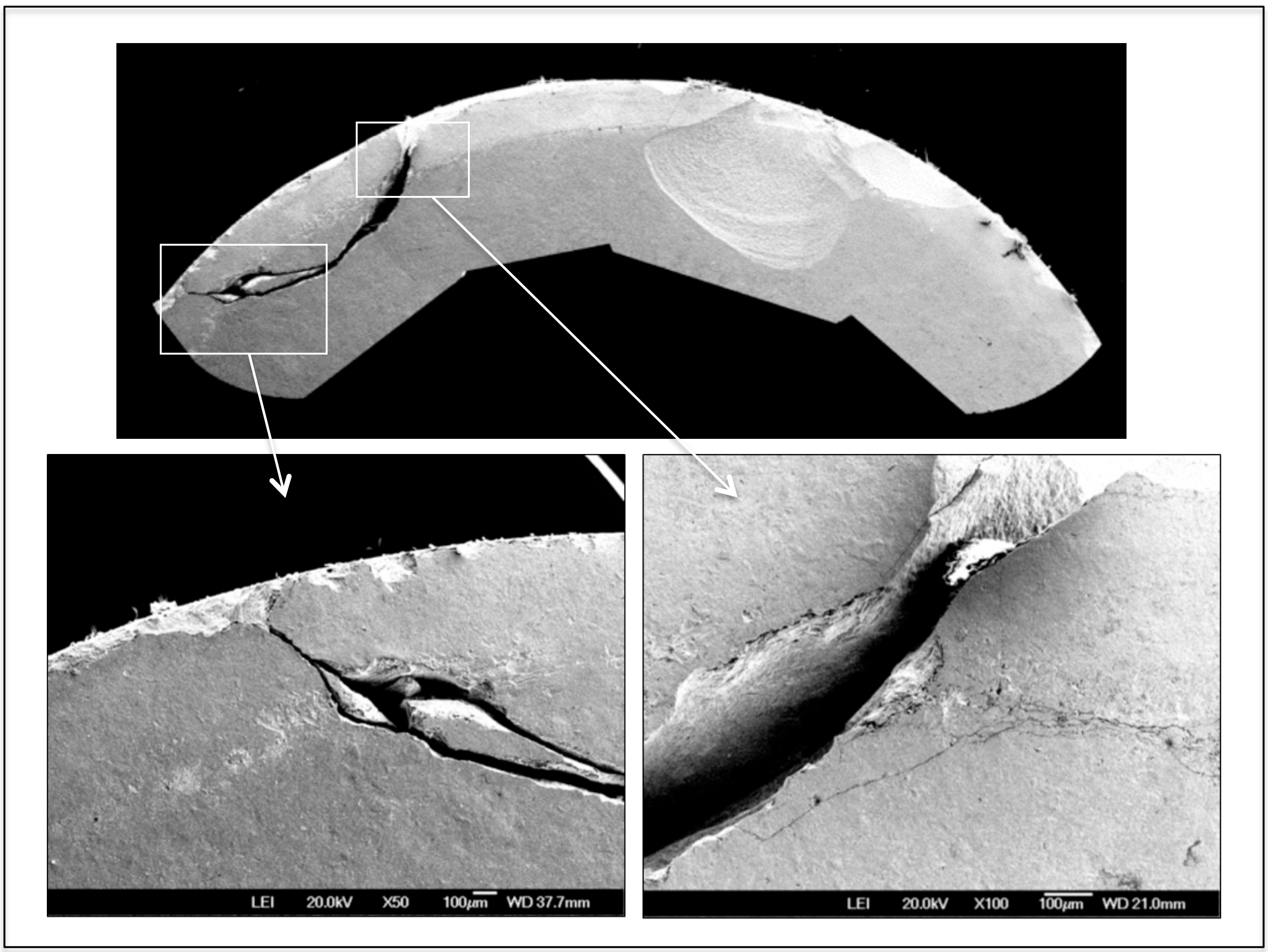

Figure 3   SEM images of the crack origin area in Pellet 11, Element 16, Bundle A.

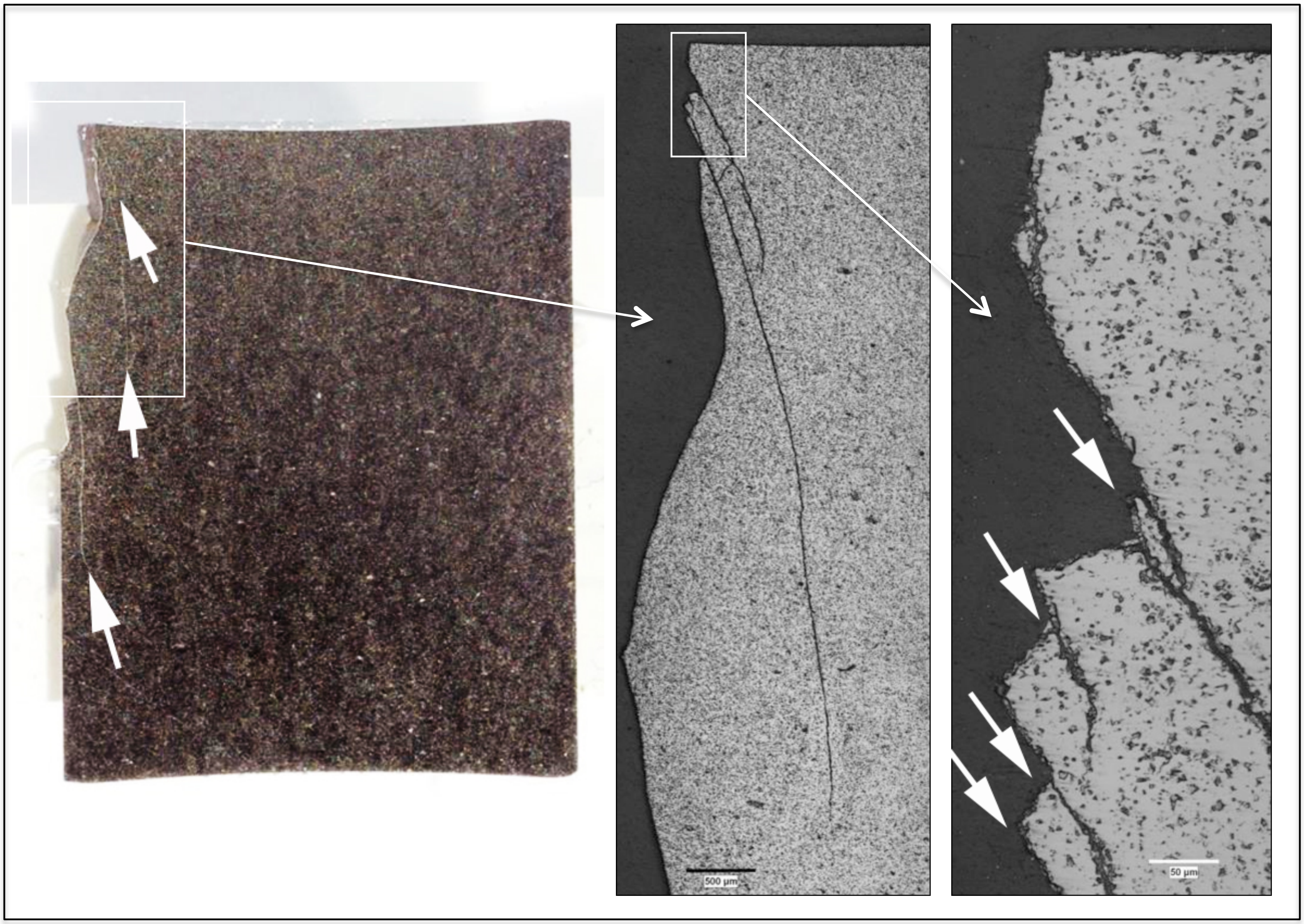

Figure 4 Polished cross-section through Pellet 10 from Element 5, Bundle B.

Figure 5 displays images of Pellet 1, Element 1 and Pellet 1, Element 6 from bundle C, which was manufactured in 2002. The fracture surfaces of these two pellets were quite different from those observed in bundles A and B manufactured in 2013 and 2012, respectively. First, the Bundle C fracture surfaces were oriented transverse to the major axis of the pellet (i.e., normal to the orientation of the axial cracks). Secondly, these fractures initiated at internal locations and propagated radially outward towards the cylinder surfaces.

Figure 6 presents detailed SEM images of the fracture surface of Element 1, Pellet 1. The UO_2 in the origin area at the core of the pellet displayed a duplex microstructure comprising small pockets of fine, granular, rounded grains and voids within a matrix of larger, faceted crystals. Some small secondary cracks were observed within this duplex microstructural region. Similar fracture surface features were observed at the origin area of Element 6, Pellet 1 when examined by SEM.

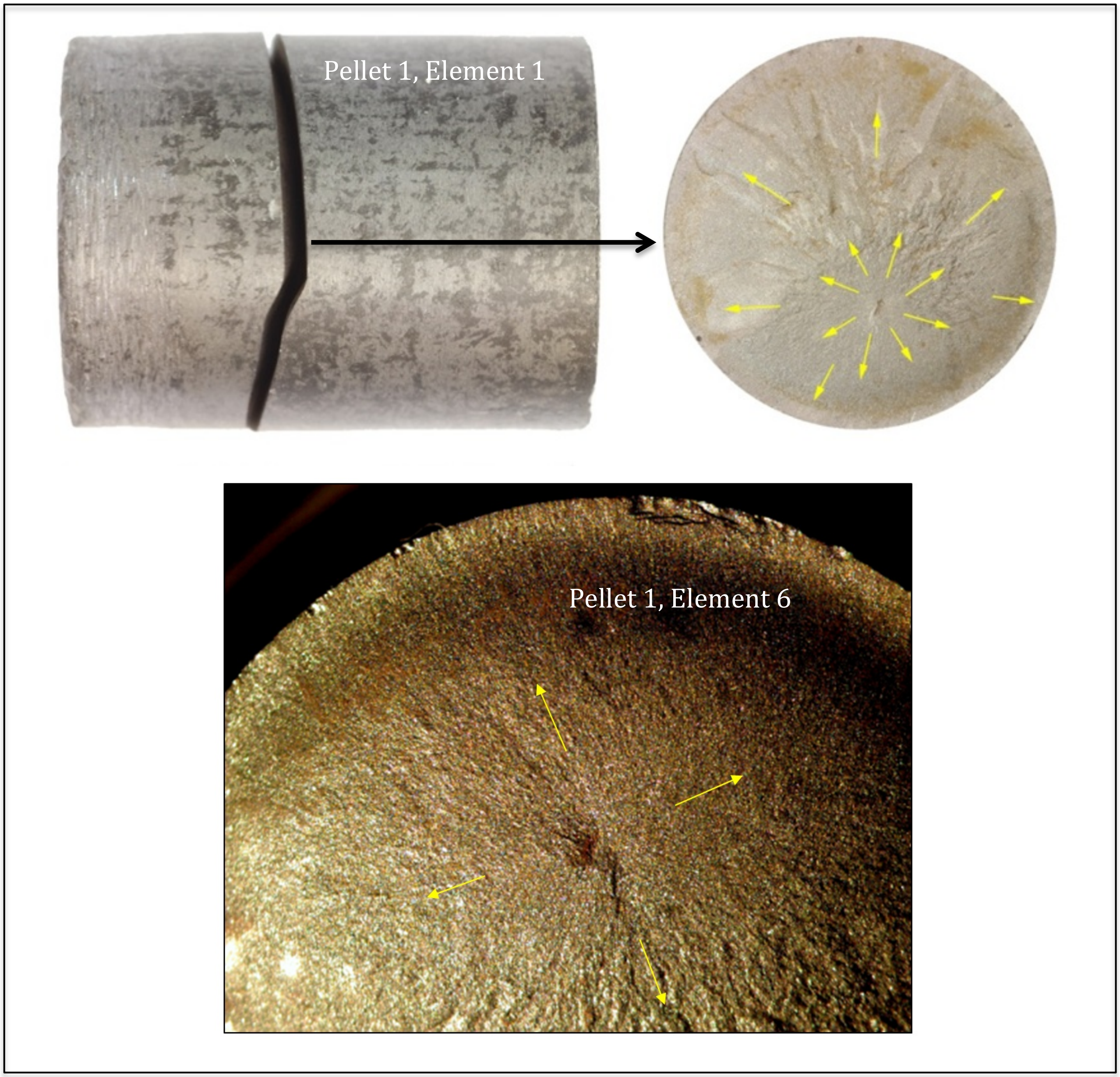

Figure 5 Crack origin area and propagation directions of two pellets from Bundle C.

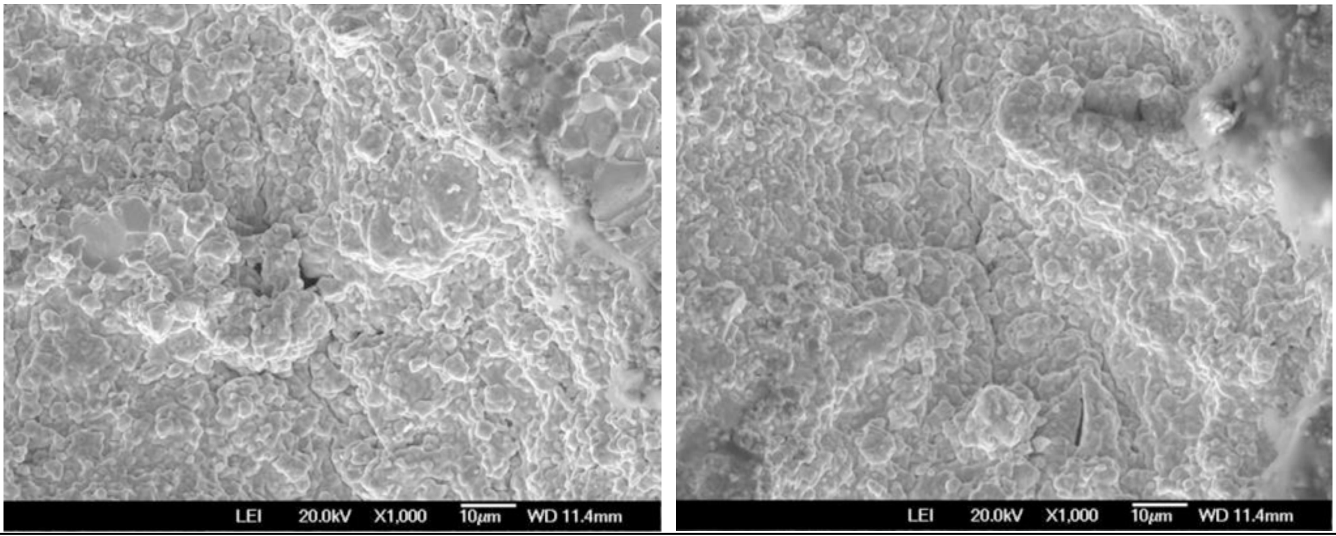

Figure 6 SEM images of the crack origin area of Pellet 1, Element 1 from Bundle C.

Figure 7 is a polished cross-section specimen through the origin area of Element 1, Pellet 1. The UO_2 displayed elevated levels of porosity at this location. A small transverse secondary crack can also be observed beneath the main fracture surface that spans several of the small pores in the UO_2.

Porosity measurements were obtained from the core region of all of the pellets described above, plus two others from Bundles A and B. The results of these measurements, presented in Table 1, indicate that the porosity levels for pellets from Bundles A and C were significantly higher than those for the two pellets examined from Bundle B. Based on the theoretical density of UO_2 (10.96 g/cc), the maximum core porosity levels in the pellets from Bundles A and C correspond to local densities between 9.12 g/cc and 9.91 g/cc. These values were below the design specification range for the *bulk density* of the UO_2 pellets (measured using the Archimedes method) of 10.45 g/cc to 10.75 g/cc. In contrast, the maximum core porosity levels in the pellets from Bundle B correspond to densities between 10.46 g/cc and 10.67 g/cc, which fall within the specification range. These estimates are in general agreement with data collected by Stern Laboratories, which showed that the weight distribution for the new bundles was higher than the old bundles for both the long and standard length bundles.

Table 1 – Microstructural Measurements of Porosity at the UO_2 Fuel Pellet Core

Bundle	**A**	**A**	**A**	**B**	**B**	**C**	**C**
Element	**16**	**16**	**16**	**5**	**5**	**1**	**6**
Pellet	**25**	**26**	**31**	**10**	**12**	**1**	**1**
Year Manufactured	**2013**	**2013**	**2013**	**2012**	**2012**	**2002**	**2002**
Average Porosity	**15.6%**	**11.7%**	**12.5%**	**2.6%**	**4.6%**	**9.5%**	**16.7%**
Estimated Local Density (g/cc)	9.25	9.67	9.59	10.67	10.46	9.91	9.12
Bulk Density Design Specification (g/cc)	10.60 ± 0.15						

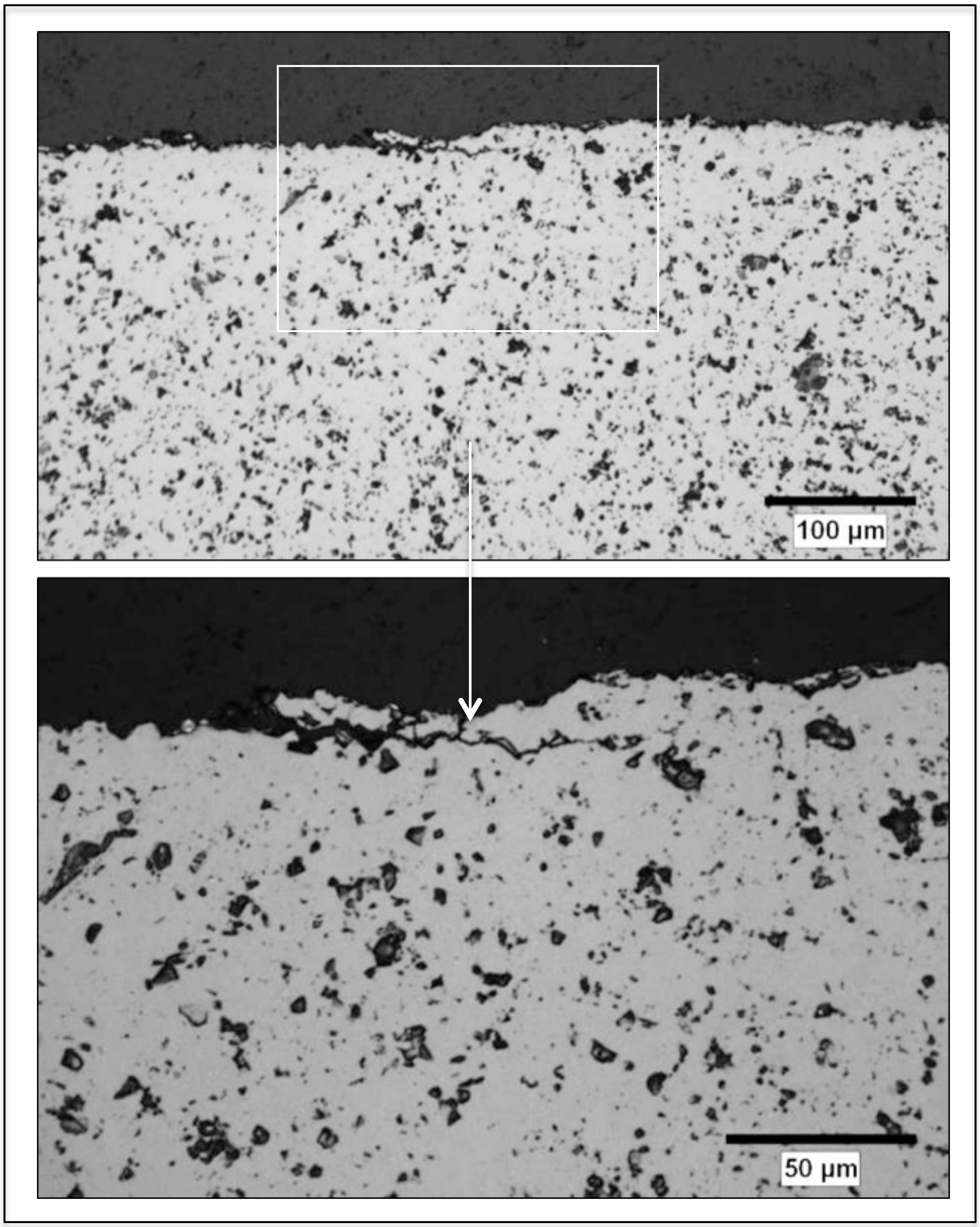

Figure 7 Polished cross-section through the crack origin area of Pellet 1, Element 1 from Bundle C.

3. Discussion

The damaged UO_2 fuel pellets displayed two basic fracture surface orientations:

(1) Axially-oriented cracks that initiated on the rims of the pellets led to the break-out of material from the sides of the cylinders. These cracks were observed in pellets removed from recently manufactured fuel bundles (i.e., pellets from Bundles A and B).
(2) Cracks that initiated at pockets of porosity in the pellet core and resulted in fractures that were transverse to the cylindrical axis of the pellets. These cracks were unique to the pellets manufactured circa 2002 (i.e., pellets from Bundle C).

The fuel pellets with large fractures (both axial and transverse) displayed elevated levels of internal porosity (i.e., up to ~16 vol%) with corresponding local densities that were below the bulk material specification range (i.e. as low as 9.12 g/cc versus the manufacturer's lower limit of 10.45 g/cc). The large polygonal pores and low local densities observed in the fractured UO_2 fuel pellets are features typically associated with a sintering defect known as 'solarization' [3]. Solarization is usually caused by high heating ramp rates and high sintering temperatures. Some alternative explanations for the observed high porosity levels in these pellets are non-uniform die compaction and incomplete sintering. The reduced local densities and possible residual stresses within these pellets would make them more fragile and susceptible to cracking under applied mechanical loads.

The geometry of the pellet rim in the area where the axial cracks initiated in pellets from Bundles A and B is not well defined in design drawings. This could be contributing to localized variations in the pellet-to-pellet contact area and stress. The reported tight fit of pellets in the fuel sheaths plus the application of manual loads, when combined with the material and dimensional issues noted above, may create conditions that are favourable to axial cracking as the pellet stacks are assembled into the fuel element sheaths. The mirroring and replication of axial cracks along one side of adjacent and nearby pellets suggests that local stress concentrations may be caused by the misalignment or bending of the pellet stack as it is being axially compressed. This might occur if the motion of the pellet stack was momentarily impeded (e.g. due to local pellet-to-sheath clearance issues) during element loading under the applied axial force. For the pellets that were manufactured in 2002, residual sintering stresses may have contributed to the development of transverse cracks that initiated at internal porosity defects.

It should be noted that Bundle C (2002) was previously used for other experiments at Stern Laboratories. The extent to which this particular bundle was used in previous experiments is not fully known but they would have involved thermal and mechanical testing. Hence for Bundle C the defects found are not necessarily related to manufacturing issues alone, whereas the new fuel bundles were shipped to Stern Laboratories directly from Darlington stores and have no previous history of testing.

Our previous paper [1] discussed the observation that fuel bundle masses have been increasing since 2002. Further investigations have verified the observed increasing trend in both fuel pellet bulk densities and in total bundle masses. In addition, additional inspections of previously inaccessible fuel bundles have permitted the observation that the majority of defected bundles were found to have manufacturing serial numbers within two relatively narrow ranges, 2786 bundles in one set (2012) and 4713 bundles in the other (2010). These represent small fractions of the approximately 23,000 fuel bundles used at Darlington each year.

We have also observed that these defected bundles have consistently been among the heavier bundles irradiated at Darlington. This is demonstrated in Figure 8. All of the defected bundles of the 37R Long design were found to reside above the mean of the mass distribution of 15,000 sequentially numbered fuel bundles. This pattern is also observed with the 37M Long bundles , although in this case, two defected bundles are positioned below the mean. This is not unexpected since the 37M design is a recent innovation, with production dates well after the increasing trends in bundle mass and pellet densities were established.

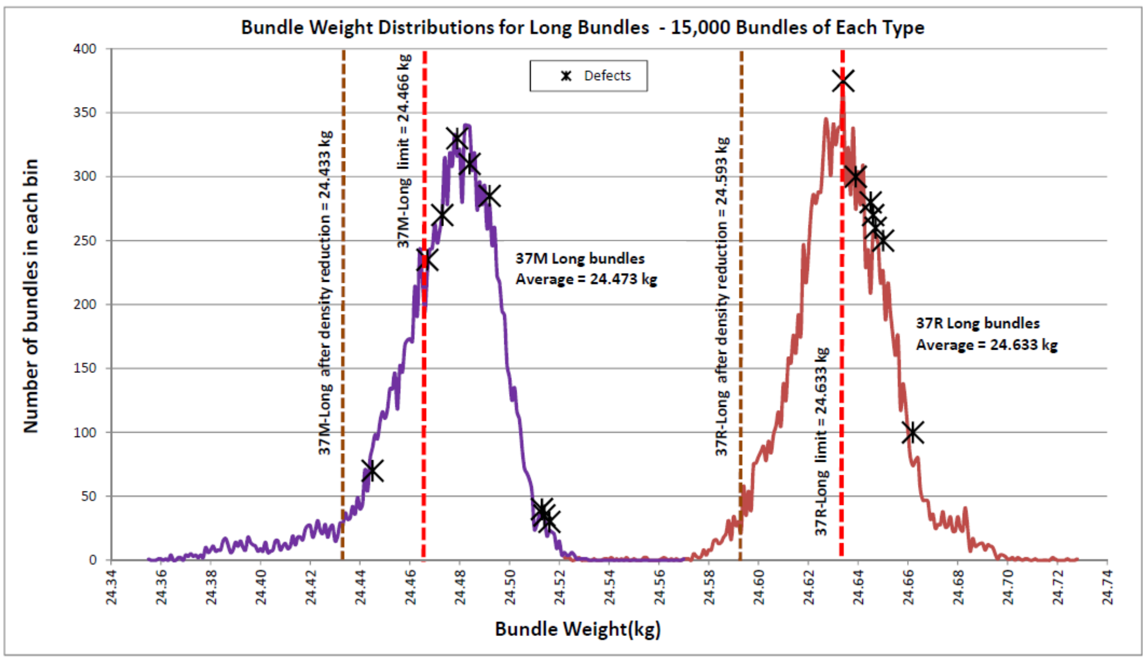

Figure 8 – Weight distributions for 37R and 37M long bundles including defected bundles

OPG adheres to a "zero fuel defect" policy and responded energetically to this fuel defect excursion. The response and recovery plan discussed in our previous paper [1] has been implemented. Figure 8 includes the operational "loading limits" which were discussed in that paper. In addition, OPG and the fuel manufacturer have implemented a number of adjustments to fuel manufacturing parameters to increase fuel pellet to fuel sheath clearances and to reduce the chances of pellet to cladding interactions during pellet loading. These "adjustments" were minor and within the existing approved fuel design envelope, and are; (1) reduction in the target fuel pellet density by 0.022 g/cm^3, returning densities to pre 2003 values, (2) reduction in pellet diameters by 10 µm to 20 µm in an effort to eliminate interference between pellet and fuel sheath during loading of fuel pellets, (3) introduction of controls to limit the applied force during manual loading of fuel pellet stacks into fuel sheaths.

Recent destructive examinations of the heaviest of these "adjusted" bundles have revealed much lower levels of pellet damage than discussed in this paper. The "adjusted" fuel bundles have been gradually phased into use at Darlington since late December 2014, and are now being used in all units. The four Darlington reactors are currently operating free of fuel defects.

4. Conclusions

The microscopic pellet examinations discussed in this paper as well as several other investigations conducted by OPG has led to the following working hypothesis concerning the cause of the Darlington fuel defect excursion. We hypothesize that a combination of pellet fragility, inadequate internal clearances and high loading forces led to pellet fracture during loading into fuel sheaths and to internal sheath damage by pellet fragments. These weakened fuel elements may have been more prone to failure, especially if subjected to the highest high power ramp for Darlington reactors in nominal configuration, fuel shifting from Position 2 to Position 6. It is very likely that intact fuel sheaths and elements were less susceptible to failure. The robustness of the Darlington fuel design with respect to fuelling power ramps has been validated by over 20 years of operation without defects attributable to power ramps [1]. The occurrence of these defects during two relatively narrow manufacturing "clusters" support the validity of our hypothesis, indicating that at times a convergence of adverse manufacturing parameters (e.g. fragile pellets and low internal clearances) can lead to a susceptible lot of fuel bundles.

5. References

[1] J. Judah and S. Goodchild, "Assessment of the Causes for Degrading Fuel Performance at Darlington NGS", Paper No. 88 presented at the 12th International Conference on CANDU Fuel, Kingston, Ontario, Canada, 2013 September 15-18, 25 pp.

[2] J. R. Varner, "Fracture Modes and Appearances in Ceramics", in Failure Analysis and Prevention, ASM Handbook, Volume 11, ASM International, Materials Park, OH, 2002, pp. 662-670.

[3] A. Marajofsky, "On the Sintering Kinetics in UO_2", in Advances in Fuel Pellet Technology for Improved Perfromance at High Burnup, IAEA-TECDOC-1036, International Atomic Energy Agency, Vienna, 1998, pp. 41-48.